УДК 624.048-033.26.621.55

M.B. Demchuk, O.G. Nakonechnyi
National University of Water Management and Natural Resources Use,
Applied Mathematics Department

INJECTION FRONT INTERPOLATION IN REAL SCALE GROUTING MODELS

Виконана числова перевірка того, що невизначеністю у кінцевому положенні фронту нагнітання, зумовленою невизначеністю у виборі методу інтерполювання фронту нагнітання на кожному часовому шарі, можна знехтувати, оцінюючи похибку методу розрахунку цього положення у моделі промислової цементації ґрунту. Результати числових експериментів вказують на те, що криволінійна сітка, на якій виконується розрахунок, має хаотичні розміщення своїх вузлів на деяких часових шарах і що це не призводить до істотного спотворення кінцевого положення фронту нагнітання.

Ключові слова: фронт нагнітання, інтерполювання, цементація ґрунту.

It is checked numerically that the uncertainty in the final injection front position due to uncertainty in the choice of the method of the injection front interpolation on every time layer can be neglected in the estimation of the truncation error of the calculation of this position in the framework of the real scale grouting model. Results of numerical experiments indicate that the curvilinear grid this calculation is performed on has chaotic dispositions of its nodes in space on some time layers and that it does not give rise to significant final injection front position distortion.

Key words: injection front, interpolation, scale grouting model.

Introduction

Strengthening a soft ground must precede the tunnel construction in it to have enough time for installing needed support. Permeation grouting is a technique widely used for this soil reinforcement [1]. It consists in injecting into a soil a cement grout at a constant pressure or a constant pumping rate. Grouting is rather costly and time consuming. Its regime is determined by cement concentration distribution evolution [2]. Therefore, a calculation of this evolution using mathematical modeling is important.

There are a lot of papers, for instance [2–4], in which a standard laboratory test is modeled to shed light on various issues of the mathematical description of cement grout propagation in a porous medium. In this test a cement grout is injected at a constant pumping rate in the base of a vertical tube opened at the top and filled with water saturated sand. The problem set ups [5–7] correspond to *in situ* grouting. The continuum grouting models [2–7] can be referred to the class of problems about pollution propagation, and the formulations of these models take advantage of different sets of assumptions that simplify the system containing the porous medium and the infiltrate. Specifically, in [3, 4, 6, 7] the ground skeleton is regarded as absolutely rigid while in [2, 5] it is assumed to be deformable. In [7] the hydromechanical dispersion and diffusion are neglected. In [3, 6] it is assumed that cement particles are large enough to be trapped by small pore throats; conversely in [2, 5, 7] it is assumed and that they are much smaller than pore throats and that they deposit over pore throats and pore bodies. Demchuk [4] assumes that cement particles can not be trapped by pore throats and that they do not deposit over pore throats and pore bodies. Demchuk [8, 9] neglects peculiarities of grout propagation in a porous medium and describes the real scale grouting by the model that belongs to the class of problems with free moving boundaries. In [8, 10] the continuum real scale grouting models of this type are presented. However, Demchuk [11] shows that the continuum

approach was not properly adopted in them and modifies numerical modeling [8], [10] to guarantee the appropriateness of applying this approach. A comparison of model calculations with measurements verifies the set of assumptions used in the model formulation. The amount of information it provides depends on values of uncertainties in the compared quantities [4]. In the models [2–7] the sought functions contain high gradient regions which positions change as time goes and are not known in advance. Therefore, to estimate truncation errors of calculations in the frameworks of these models one is supposed to conduct the analysis of numerical solutions [4]. The main drawback of the models [2, 3, 5–7] is that calculations in their frameworks require significant computer resources. Demchuk [4] explains this by the fact that each one of these models is a system of differential equations in partial derivatives with initial and boundary conditions that do not conform to each other and presents the standard laboratory test model that does not have this drawback. Demchuk and Saiyouri [12] describe the method of a realization of the uncertainty uniformity principle in calculations in the framework of the model [4]. It should be noted that the curvilinear grid Demchuk [11] performs calculations on can have chaotic disposition of its nodes in space on some time layers [9]. However, Demchuk [11] checks numerically that this fact does not give rise to inconsistencies between results of these calculations. Hence, the finite difference schemes according to which Demchuk [11] performs calculations are conditionally stable. Therefore, round off errors of these calculations are negligible. Demchuk [11] estimates the truncation errors of the final injection front position calculations using the assumption that contributions of uncertainties in these positions due to uncertainties in the choices of methods of injection front interpolations on every time layer to these errors are negligible. The goal of this work is to check this assumption numerically.

Numerical modeling of a real scale cement grout injection in a dry soil

In this work we consider four problem set ups [11]. In the cases of set ups # 1 and # 3, we assume that a long trench is made under an injector foundation. Its width is $2 \cdot r_0$, and its depth is h_0. The astringent infiltrate is injected in this trench at the constant pressure p_0 (see Figure 1 (a)). In set ups # 2 and # 4 we have a round bore-hole instead of the trench and assume that other conditions are the same. Its radius is r_0, and its depth is h_0. In the first two set ups the ground skeleton is regarded as absolutely rigid, while in the last two ones it is assumed to be deformable. In each case, the injection front (the curve Γ_4 on Figure 1 (a)) is a free surface and its evolution in time and space needs to be found.

Demchuk [11] divides continuum real scale grouting models that belong to the class of problems with free moving boundaries into two types. In the models of the first type at each moment of time t Demchuk [11] performs numerical modeling in the curvilinear quadrangle [13] $G(t)$ bounded on Figure 1 (a) by Γ_i where $i = \overline{1,4}$. In this modeling on every time layer the domain G is covered with the scanty curvilinear grid and the truncation error of the numerical calculation of the final injection front position is estimated on the basis of the analysis of the numerical solutions. In this analysis the measure of a difference between two splines $f_1(y)$ and $f_2(y)$ that interpolate final injection front positions is estimated as

$$\varepsilon = \max_{y \in [0, L]} |f_1(y) - f_2(y)| \Big/ \sqrt{y^2 + (f_1(y))^2} \ . \qquad (1)$$

In Eq. (1) $L = \max\left\{y_1^{\max}, y_2^{\max}\right\}$ where $y_1^{\max}$ and $y_2^{\max}$ are the smallest positive ordinates that satisfy $f_1\left(y_1^{\max}\right) = 0$ and $f_2\left(y_2^{\max}\right) = 0$. In the models of this type that correspond to set ups # 3 and # 4 the truncation error is approximately equal to the uncertainty in the final injection front position due to finiteness of increments of the above mentioned curvilinear grid. Each model of the second type corresponds either to set up # 3 or to set up # 4. Since information about injection front motion spreads with the aid of sound waves quickly faded due to the friction between the soil and the infiltrate, in models of this type Demchuk [8] assumes that the curve $\tilde{\Gamma}_3$ in the domain G and the moment of time t_0 starting from which piezometric head in points of this curve does not depend upon time can be chosen. In models

of this type numerical modeling is performed in $G(t)$ if $t \le t_0$. However, if $t > t_0$, it is performed in the curvilinear quadrangle $\tilde{G}(t)$ bounded on Figure 1 (a) by $\tilde{\Gamma}_i$ where $i = \overline{1,3}$ and the curve Γ_4. In each one of these models, the curve $\tilde{\Gamma}_3$ divides the respective domain $G(t_0)$ approximately in half; and Demchuk [11] chooses the moment of time t_0 to make the uncertainty in the final injection front position due to finiteness of increments of the curvilinear grid and the measure of the difference between the final injection front position and the one calculated in the framework of the respective model of the first type calculated according to Eq. (1) to be as small as possible. Since Demchuk [11] assumes that contributions of uncertainties in final free surface positions due to uncertainties in the choices of methods of injection front interpolations on every time layer to the truncation errors are negligible, the fact that the moment of time t_0 can be chosen as described in each case Demchuk [11] considers verifies this assumption. The shapes of $G(t)$ and $\tilde{G}(t)$ are complicated. Therefore, Demchuk [11] seeks the numerical solutions employing the finite difference method with a usage of numerical conformal mapping. In this method on every time layer the algorithm of numerical finding of the conformal change of variables

$$x = x(\xi, \eta, t), \quad y = y(\xi, \eta, t) \tag{2}$$

that maps the curvilinear quadrangle in which the numerical modeling is performed on the parametric rectangle $R(t)$ depicted on Figure 1 (b) is used [9]. In this algorithm it is assumed that on every time layer $R(t)$ is covered with a uniform grid. The transformation defined by Eqs. (2) maps the nodes of this grid into the nodes of the curvilinear grid. The above mentioned finding consists in the determination of positions of these curvilinear grid nodes in space. Demchuk [9] finds the Cartesian coordinates of these positions solving the algebraic equation system that in the general case has the infinite number of solutions. Therefore, on some time layers this algorithm can generate the curvilinear grids with chaotic node dispositions. Demchuk [11] performs calculations on scanty grids. Therefore, approximation errors of the final injection front position calculations in the frameworks of the models [11] are significant. For each one of these models Demchuk [11] checks numerically the following assumptions. On every time layer within the

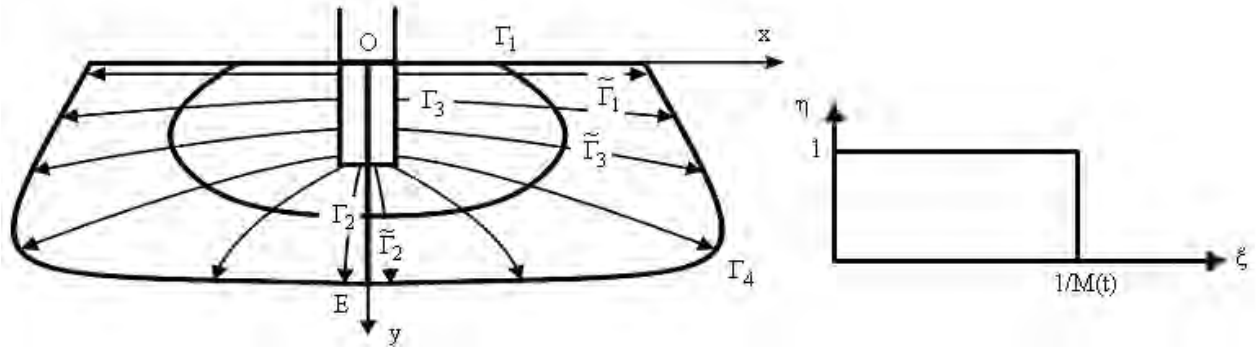

a *b*

Fig. 1 (a): The curvilinear quadrangles $G(t)$ and $\tilde{G}(t)$; (b) The parametric rectangle R(t)

limits of the approximation error the injection front can be treated as a plot of the single-valued function $x = f(y)$ which all derivatives up to the second order are continuous (hypothesis # 1). All angles at the apices of the curvilinear quadrangle in which the numerical modeling is performed are right within the limits of the approximation error (hypothesis # 2). The chaos in space dispositions of nodes of this grid on some time layers does not cause a significant distortion of the final injection front position (hypothesis # 3).

Free surface interpolation

Let us assume that we know the values of the interpolated function $f(y_p)$ in the nodal points y_p where $p = \overline{0,n}$ lying on the segment $[a, b]$ on which the injection front is interpolated. In what follows

$[A]$, $[B]$, $[\tilde{A}]$, and $[\tilde{B}]$ denote such the vectors $[A]=(y_0, y_1, \ldots, y_n)$, $[B]=(f(y_0), f(y_1), \ldots, f(y_n))$, $[\tilde{A}]=(\tilde{y}_0, \tilde{y}_1, \ldots, \tilde{y}_n)$ where $\tilde{y}_i = y_0 + y_n - y_{n-i}$, $i=\overline{0,n}$, $[\tilde{B}]=(f(y_n), f(y_{n-1}), \ldots, f(y_0))$. According to hypothesis # 2 $f'(a)=0$, $f'(b)=-N$ where N is a sufficiently large positive number.

Remark 1. According to hypothesis # 2 the derivative of the function $f(y)$ at $y=0$ equals zero within the approximation error limits (see Figure 1 (a)). From the symmetry considerations we can conclude that the values of the function $f(y)$ in the vicinity of the point $y=0$ are distorted due to gravity.

If k and m are non-negative integers such that $0 \le k \le n-m$, then we can introduce such the notations $[F_k^{(m)}]=(f(y_k), f(y_{k+1}), \ldots, f(y_{k+m}))$, $[Y_k^{(m)}]=(y_k, y_{k+1}, \ldots, y_{k+m})$, $[\tilde{F}_k^{(m)}]=(f(y_{n-k}), f(y_{n-k-1}), \ldots, f(y_{n-k-m}))$, $[\tilde{Y}_k^{(m)}]=(\tilde{y}_k, \tilde{y}_{k+1}, \ldots, \tilde{y}_{k+m})$ where $\tilde{y}_i = y_0 + y_n - y_{n-i}$, and $i=\overline{0,n}$. In what follows $P_m\left(y, [F_k^{(m)}], [Y_k^{(m)}]\right)$ denotes the interpolation polynomial [14] constructed using the values of the interpolation function $f(y_k)$, $f(y_{k+1})$, …, $f(y_{k+m})$ in the nodes y_k, y_{k+1}, …, y_{k+m}. Noting that Demchuk [11] calculates the unit vector normal to the free surface at every nodal point on every time layer and that $[Y_0^{(n)}]=[A]$, in what follows we assume that $0 < s \le n-1$. If interpolation nodes are arranged in the order of increasing $(a = y_0 < y_1 < \ldots < y_n = b)$, then we determine the piece-wise polynomial local spline $\varphi(y, s, j, [A], [B])$ where j is an integer and $0 \le j \le s$ which all derivatives up to the order s are continuous on the segment $[a, b]$ as follows

$$\varphi(y, s, j, [A], [B]) = \begin{cases} P_s\left(y, [F_0^{(s)}], [Y_0^{(s)}]\right) \text{when } y_0 \le y \le y_j, \\ Q_{2s+1,j}\left(y, [F_{k-j}^{(s+1)}], [Y_{k-j}^{(s+1)}]\right) \text{when } y \in [y_k, y_{k+1}] \\ \text{where } k = j, j+1, \ldots, n+j-s-1, \\ P_s\left(y, [F_{n-s}^{(s)}], [Y_{n-s}^{(s)}]\right) \text{when } y_{n+j-s} \le y \le y_n \end{cases}, \tag{3}$$

where $Q_{2s+1,j}\left(y, [F_{k-j}^{(s+1)}], [Y_{k-j}^{(s+1)}]\right)$ is a polynomial of a degree not greater than $2 \cdot s + 1$ determined by the following equations

$$\left.\frac{d^m Q_{2s+1,j}\left(y, [F_{k-j}^{(s+1)}], [Y_{k-j}^{(s+1)}]\right)}{dy^m}\right|_{y=y_k} = \left.\frac{d^m P_s\left(y, [F_{k-j}^{(s)}], [Y_{k-j}^{(s)}]\right)}{dy^m}\right|_{y=y_k}, \tag{4}$$

$$\left.\frac{d^m Q_{2s+1,j}\left(y, [F_{k-j}^{(s+1)}], [Y_{k-j}^{(s+1)}]\right)}{dy^m}\right|_{y=y_{k+1}} = \left.\frac{d^m P_s\left(y, [F_{k-j+1}^{(s)}], [Y_{k-j+1}^{(s)}]\right)}{dy^m}\right|_{y=y_{k+1}}, \tag{5}$$

where $k=\overline{j, n+j-s-1}$, $m=\overline{0,s}$.

Theorem 1. There is one and only one polynomial of degree not greater than $2 \cdot s + 1$ that satisfies Eqs. (4) and (5).

Proof. Rabenkii [14] proves this theorem assuming that $j=\overline{0,s-1}$. The fact that $j \ne s$ is not used in that proof. Therefore, this theorem also holds if $j = s$.

Theorem 2. If $f(y)$ is a polynomial of a degree not greater than s, then the function $\varphi(y, s, j, [A], [B])$ determined by Eq. (3) coincides with this polynomial.

Proof. If $j > 0$ and $y_0 \le y \le y_j$, then due to the uniqueness of the interpolation polynomial $\varphi(y, s, j, [A], [B]) = P_s\left(y, \left[F_0^{(s)}\right], \left[Y_0^{(s)}\right]\right) = f(y)$. If $j < s$ and $y_{n+j-s} \le y \le y_n$, then due to the uniqueness of the interpolation polynomial $\varphi(y, s, j, [A], [B]) = P_s\left(y, \left[F_{n-s}^{(s)}\right], \left[Y_{n-s}^{(s)}\right]\right) = f(y)$. Let us prove that $\varphi(y, s, j, [A], [B]) = f(y)$ when $y_k \le y \le y_{k+1}$ where $k = j, j+1, \ldots, n+j-s-1$. Due to the uniqueness of the interpolation polynomial $P_s\left(y, \left[F_{k-j}^{(s)}\right], \left[Y_{k-j}^{(s)}\right]\right) = P_s\left(y, \left[F_{k-j+1}^{(s)}\right], \left[Y_{k-j+1}^{(s)}\right]\right) = f(y)$. If we substitute $f(y)$ for $Q_{2s+1,j}\left(y, \left[F_{k-j}^{(s+1)}\right], \left[Y_{k-j}^{(s+1)}\right]\right)$ in Eqs. (4) and (5), then these equations will hold. Therefore, according to Theorem 1 $Q_{2s+1,j}\left(y, \left[F_{k-j}^{(s+1)}\right], \left[Y_{k-j}^{(s+1)}\right]\right) = f(y)$. The theorem is proved.

Theorem 3. If the function $\varphi(y, s, j, [A], [B])$ is determined by Eq. (3), then its value in the interpolation node y_p coincides with the value of the interpolated function in this node $f(y_p)$ where $p = \overline{0, n}$ and $\partial^s \varphi(y, s, j, [A], [B]) / \partial y^s$ is continuous on the segment $[a, b]$.

Proof. Since $0 < s \le n-1$, $0 \le j \le s$, the theorem will be proven if we prove it for such the values of j: $j = 0$, $0 < j < s$, and $j = s$. Firstly, we consider the case $j = 0$. In this case, according to Eq. (3) if $y \in [y_k, y_{k+1}]$ where $k = \overline{0, n-s-1}$, then $\varphi(y, s, 0, [A], [B]) = Q_{2s+1,0}\left(y, \left[F_k^{(s+1)}\right], \left[Y_k^{(s+1)}\right]\right)$; and if $y \in [y_{n-s}, y_n]$, then $\varphi(y, s, 0, [A], [B]) = P_s\left(y, \left[F_{n-s}^{(s)}\right], \left[Y_{n-s}^{(s)}\right]\right)$. Therefore, $\partial^s \varphi(y, s, 0, [A], [B]) / \partial y^s$ is continues on the segment $[y_{n-s}, y_n]$; and if $y = y_p$ where $p = \overline{n-s, n}$, then $\varphi(y_p, s, 0, [A], [B]) = f(y_p)$. If $k = \overline{0, n-s-1}$, then from Eqs. (4), (5) it follows that $\varphi(y_k, s, 0, [A], [B]) = f(y_k)$ and that $\partial^s \varphi(y, s, 0, [A], [B]) / \partial y^s$ is continues on the segment $[a, b]$. In the case $0 < j < s$, according to Eq. (3) if $y \in [y_0, y_j)$, then $\varphi(y, s, j, [A], [B]) = P_s\left(y, \left[F_0^{(s)}\right], \left[Y_0^{(s)}\right]\right)$; if $y \in [y_k, y_{k+1}]$ where $k = \overline{j, n+j-s-1}$, then $\varphi(y, s, j, [A], [B]) = Q_{2s+1,j}\left(y, \left[F_{k-j}^{(s+1)}\right], \left[Y_{k-j}^{(s+1)}\right]\right)$; and if $y \in [y_{n+j-s}, y_n]$, then $\varphi(y, s, j, [A], [B]) = P_s\left(y, \left[F_{n-s}^{(s)}\right], \left[Y_{n-s}^{(s)}\right]\right)$. Therefore, $\partial^s \varphi(y, s, j, [A], [B]) / \partial y^s$ is continuous on $[y_0, y_j) \cup (y_{n+j-s}, y_n]$ and if $y = y_p$ where $p = \overline{0, j}, \overline{n+j-s, n}$, then $\varphi(y_p, s, j, [A], [B]) = f(y_p)$. If $k = \overline{j, n+j-s-1}$, then from Eqs. (4), (5) it follows that $\varphi(y_k, s, j, [A], [B]) = f(y_k)$ and that $\partial^s \varphi(y, s, j, [A], [B]) / \partial y^s$ is continuous on the segment $[a, b]$. In the case $j = s$, according to Eq. (3) if $y \in [y_0, y_s]$, then $\varphi(y, s, s, [A], [B]) = P_s\left(y, \left[F_0^{(s)}\right], \left[Y_0^{(s)}\right]\right)$; and if $y \in [y_k, y_{k+1}]$ where $k = \overline{s, n-1}$, then $\varphi(y, s, s, [A], [B]) = Q_{2s+1,0}\left(y, \left[F_{k-j}^{(s+1)}\right], \left[Y_{k-j}^{(s+1)}\right]\right)$. Therefore, $\partial^s \varphi(y, s, s, [A], [B]) / \partial y^s$ is continues on $[y_0, y_s]$ and if $y = y_p$ where $p = \overline{0, s}$, then $\varphi(y_p, s, s, [A], [B]) = f(y_p)$. If $k = \overline{s, n-1}$, then from Eqs. (4), (5) it follows that $\varphi(y_k, s, s, [A], [B]) = f(y_k)$, $\varphi(y_n, s, s, [A], [B]) = f(y_n)$, and that $\partial^s \varphi(y, s, s, [A], [B]) / \partial y^s$ is continues on the segment $[a, b]$. The theorem is proved.

In what follows unless otherwise specified we assume that $n > 5$.

Definition 1. The spline $\varphi(y, s, j, [A], [B])$ is strongly local in the vicinity of the point $y = a$ (the point $y = b$) if the following holds. If $y \in [y_0, y_s]$ $(y \in [y_{n-s}, y_n])$, then $\varphi(y, s, j, [A], [B])$ does not depend on y_{s+i+1} and $f(y_{s+i+1})$ (y_i and $f(y_i)$) where $i = \overline{0, n-s-1}$.

Remark 2. From Eq. (3) it follows that if $y \in [y_0, y_3]$ $(y \in [y_{n-3}, y_n])$, then for each integer j such that $0 \le j \le 3$ $\varphi(y, 3, j, [A], [B])$ depends only on y, y_i, and $f(y_i)$ where $i = \overline{0, 6-j}$ $\left(i = \overline{n-3-j, n}\right)$. Thus, according to Definition 1 the spline $\varphi(y, 3, 3, [A], [B])$ is strongly local in the vicinity of the point $y = a$ while the spline $\varphi(y, 3, 0, [A], [B])$ is strongly local in the vicinity of the point $y = b$. From Definition 1 and Theorem 2 it follows that in the general case the splines $\varphi(y, 3, j, [A], [B])$ where $j = \overline{0,2}$ are not strongly local in the vicinity of the point $y = a$ while the splines $\varphi(y, 3, j, [A], [B])$ where $j = \overline{1,3}$ are not strongly local in the vicinity of the point $y = b$.

It is convenient to introduce such the change of variables

$$\tilde{y} = a + b - y \tag{6}$$

and such the numbering of the points in which the interpolation nodes are mapped by it

$$\tilde{y}_p = a + b - y_{n-p}, \tag{7}$$

where $p = \overline{0, n}$. We determine the function $\tilde{f}(\tilde{y})$ in the following way

$$\tilde{f}(\tilde{y}) = f(a + b - \tilde{y}). \tag{8}$$

Theorem 4. The following equalities hold

$$\varphi(y, 1, 1, [A], [B]) = \varphi(\tilde{y}, 1, 0, [\tilde{A}], [\tilde{B}]), \tag{9}$$

$$\varphi(y, 2, 2, [A], [B]) = \varphi(\tilde{y}, 2, 0, [\tilde{A}], [\tilde{B}]), \quad \varphi(y, 2, 1, [A], [B]) = \varphi(\tilde{y}, 2, 1, [\tilde{A}], [\tilde{B}]). \tag{10}$$

Proof. If $y_k \le y \le y_{k+1}$ where $k = \overline{0, n-1}$, then according to Eqs. (6) and (7) $\tilde{y}_{n-k-1} \le \tilde{y} \le \tilde{y}_{n-k}$. From Eqs. (6) and (7) it follows that $y - y_p = \tilde{y}_{n-p} - \tilde{y}$ where $p = \overline{0, n}$. From Eqs. (7) and (8) it follows that $\tilde{f}(\tilde{y}_p) = f(y_{n-p})$ where $p = \overline{0, n}$. From Eq. (7) it follows that $\tilde{y}_k - \tilde{y}_r = y_{n-r} - y_{n-k}$ where $k = \overline{0, n}$, $r = \overline{0, n}$. Therefore, from the explicit form of an interpolation polynomial [14] it follows that

$$P_s\left(y, \left[F_{k-s+1}^{(s)}\right], \left[Y_{k-s+1}^{(s)}\right]\right) = P_s\left(a + b - y, \left[\tilde{F}_{n-k-1}^{(s)}\right], \left[\tilde{Y}_{n-k-1}^{(s)}\right]\right) \tag{11}$$

where $k = \overline{s-1, n-1}$ and $s = \overline{1,2}$.

From Eqs. (4)–(7) it follows that

$$\left.\frac{d^m Q_{2s+1, j_s}\left(\tilde{y}, \left[\tilde{F}_{p-j_s}^{(s+1)}\right], \left[\tilde{Y}_{p-j_s}^{(s+1)}\right]\right)}{d\tilde{y}^m}\right|_{\tilde{y}=\tilde{y}_p} = \left.\frac{d^m P_s\left(\tilde{y}, \left[\tilde{F}_{p-j_s}^{(s)}\right], \left[\tilde{Y}_{p-j_s}^{(s)}\right]\right)}{d\tilde{y}^m}\right|_{\tilde{y}=\tilde{y}_p}, \tag{12}$$

$$\left.\frac{d^m Q_{2s+1, j_s}\left(\tilde{y}, \left[\tilde{F}_{p-j_s}^{(s+1)}\right], \left[\tilde{Y}_{p-j_s}^{(s+1)}\right]\right)}{d\tilde{y}^m}\right|_{\tilde{y}=\tilde{y}_{p+1}} = \left.\frac{d^m P_s\left(\tilde{y}, \left[\tilde{F}_{p-j_s+1}^{(s)}\right], \left[\tilde{Y}_{p-j_s+1}^{(s)}\right]\right)}{d\tilde{y}^m}\right|_{\tilde{y}=\tilde{y}_{p+1}} \tag{13}$$

where $s=\overline{1,2}$, $m=\overline{0,s}$, $j_1=0$, $j_2=\overline{0,1}$, $p=\overline{j_s,n+j_s-1-s}$. $Q_{2s+1,j_s}\left(\tilde{y},\left[\tilde{F}_{p-j_s}^{(s+1)}\right],\left[\tilde{Y}_{p-j_s}^{(s+1)}\right]\right)$ is a polynomial of degree not greater than $2\cdot s+1$ with respect to $\tilde{y}$ and the change of variables determined by Eq. (6) is linear. Therefore, $Q_{2s+1,j_s}\left(a+b-y,\left[\tilde{F}_{p-j_s}^{(s+1)}\right],\left[\tilde{Y}_{p-j_s}^{(s+1)}\right]\right)$ is a polynomial of degree not greater than $2\cdot s+1$ with respect to y. If $k=n-p-1$, then from Eqs. (11)–(13) it follows that

$$\left.\frac{d^m Q_{2s+1,j_s}\left(\tilde{y},\left[\tilde{F}_{n-k-1-j_s}^{(s+1)}\right],\left[\tilde{Y}_{n-k-1-j_s}^{(s+1)}\right]\right)}{dy^m}\right|_{y=y_k}=\left.\frac{d^m P_s\left(y,\left[F_{k-s+j_s}^{(s)}\right],\left[Y_{k-s+j_s}^{(s)}\right]\right)}{dy^m}\right|_{y=y_k}, \quad (14)$$

$$\left.\frac{d^m Q_{2s+1,j_s}\left(\tilde{y},\left[\tilde{F}_{n-k-1-j_s}^{(s+1)}\right],\left[\tilde{Y}_{n-k-1-j_s}^{(s+1)}\right]\right)}{dy^m}\right|_{y=y_{k+1}}=\left.\frac{d^m P_s\left(y,\left[F_{k-s+j_s+1}^{(s)}\right],\left[Y_{k-s+j_s+1}^{(s)}\right]\right)}{dy^m}\right|_{y=y_{k+1}}, \quad (15)$$

where $\tilde{y}$ is calculated according to Eq. (6), $s=\overline{1,2}$, $m=\overline{0,s}$, $j_1=0$, $j_2=\overline{0,1}$, $k=\overline{s-j_s,n-1-j_s}$. From Eqs. (4)–(6), (14), (15), and Theorem 1 it follows that

$$Q_{2s+1,s-j_s}\left(y,\left[F_{k+j_s-s}^{(s+1)}\right],\left[Y_{k+j_s-s}^{(s+1)}\right]\right)=Q_{2s+1,j_s}\left(a+b-y,\left[\tilde{F}_{n-k-1-j_s}^{(s+1)}\right],\left[\tilde{Y}_{n-k-1-j_s}^{(s+1)}\right]\right), \quad (16)$$

where $s=\overline{1,2}$, $m=\overline{0,s}$, $j_1=0$, $j_2=\overline{0,1}$, $k=\overline{s-j_s,n-1-j_s}$. From Eqs. (3), (11), and (16) it follows that Eqs. (9) and (10) hold. The theorem is proved.

If $y\in\left\lfloor y_{p-1},y_p\right\rfloor$ where $p=\overline{1,n}$, then the non-local spline $g(y,m,[A],[B])$ where $m=\overline{1,4}$ is a cubic polynomial

$$g(y,m,[A],[B])=a_p+b_p^m\left(y-y_{p-1}\right)+c_p^m\left(y-y_{p-1}\right)^2+d_p^m\left(y-y_{p-1}\right)^3, \quad (17)$$

where

$$a_p=f\left(y_{p-1}\right),\ b_p^m=\frac{f\left(y_p\right)-f\left(y_{p-1}\right)}{y_p-y_{p-1}}-\frac{2\cdot c_p^m\left(y_p-y_{p-1}\right)}{3}-\frac{c_{p+1}^m\left(y_p-y_{p-1}\right)}{3}, \quad (18)$$

$$d_p^m=\frac{c_{p+1}^m-c_p^m}{3\cdot\left(y_p-y_{p-1}\right)},\ b_n^m=\frac{3}{2}\frac{\left(f\left(y_n\right)-f\left(y_{n-1}\right)\right)}{y_n-y_{n-1}}-\frac{y_n-y_{n-1}}{2}c_n^m-\frac{D_m}{2}, \quad (19)$$

$$d_n^m=\left(f\left(y_n\right)-f\left(y_{n-1}\right)\right)/\left(y_n-y_{n-1}\right)^3-b_n^m/\left(y_n-y_{n-1}\right)^2-c_n^m/\left(y_n-y_{n-1}\right). \quad (20)$$

In the second equation of Eqs. (19) $D_m=dP_m\left(y,\left[F_{n-m}^{(m)}\right],\left[Y_{n-m}^{(m)}\right]\right)/dy\Big|_{y=y_n}$. In Eqs. (18) and in the first equation of Eqs. (19) $p=\overline{1,n}$. c_p^m where $p=\overline{1,n}$ that enter Eq. (17) satisfy the following equation system

$$2h_1c_1^m+h_1c_2^m=3\cdot\left(f\left(y_1\right)-f\left(y_0\right)\right)/h_1-3\cdot C_m, \quad (21)$$

$$h_i\cdot c_i^m+2\cdot\left(h_i+h_{i+1}\right)\cdot c_{i+1}^m+h_{i+1}\cdot c_{i+2}^m=3\left(\frac{f\left(y_{i+1}\right)-f\left(y_i\right)}{h_{i+1}}-\frac{f\left(y_i\right)-f\left(y_{i-1}\right)}{h_i}\right), \quad (22)$$

$$\frac{h_{n-1}}{3}\cdot c_{n-1}^m+\left(\frac{2}{3}h_{n-1}+\frac{h_n}{2}\right)\cdot c_n^m=\frac{3}{2}\cdot\frac{f\left(y_n\right)-f\left(y_{n-1}\right)}{h_n}-\frac{f\left(y_{n-1}\right)-f\left(y_{n-2}\right)}{h_{n-1}}-\frac{D_m}{2}, \quad (23)$$

which solution can be found by the Thomas algorithm. In Eq. (22) $i=\overline{1,n-2}$ and in Eq. (21) $C_m = dP_m\left(y, \left[F_0^{(m)}\right], \left[Y_0^{(m)}\right]\right)/dy\Big|_{y=y_0}$. In the reference [15] it is shown that

$$\partial g(y, m, [A], [B])/\partial y\big|_{y=y_0} = C_m,\ \partial g(y, m, [A], [B])/\partial y\big|_{y=y_n} = D_m, \tag{24}$$

$g\left(y_p, m, [A], [B]\right) = f\left(y_p\right)$ where $p=\overline{0,n}$; if $y\in[a,b]$, then $\partial^2 g(y, m, [A], [B])/\partial y^2$ is continuous.

Remark 3. On every time layer Demchuk [11] covers the parametric rectangle $R(t)$ depicted on Figure 1 (b) with a uniform grid. Substituting coordinates of nodes of this grid for ξ and η in Eqs. (2), we obtain the coordinates of curvilinear grid nodes. The ratio of sides a curvilinear grid cell is the conformal mapping invariant (the parameter $M(t)$ on Figure 1 (b)) [13], and the above mentioned number N is rather large. Therefore, injection front interpolation nodes are situated in the vicinity of the point E depicted on Figure 1 (a) more compactly than in the rest of the segment OE. Hence, the probability of a chaotic disposition of nodes situated in the vicinity of the point E is higher than that of other interpolation nodes. It results in possible distortion of the injection front stronger in the vicinity of the point E than in other parts of the segment OE. For simplicity, in what follows we assume that this possible distortion is not negligible only in the vicinity of the point E.

In what follows if $y_{i+1} < y_i$ where $0\le i\le n-1$, then $[y_i, y_{i+1}] = \emptyset$. We interpolate the free surface on every time layer by functions determined in the following way. Under condition $y\ge y_n$ or under conditions $y\in[y_{n-1}, y_n]$ and $y\notin[y_k, y_{k+1}]$ where $k=\overline{0,n-2}$ $\breve{\varphi}(y,1,0,[A],[B]) = P_1\left(y, \left[F_{n-1}^{(1)}\right], \left[Y_{n-1}^{(1)}\right]\right)$ otherwise if $y\in\left[y_{k_{min}}, y_{k_{min}+1}\right]$ where k_{min} is the smallest between integer numbers k such that $0\le k\le n-2$ and $y\in[y_k, y_{k+1}]$, then $\breve{\varphi}(y,1,0,[A],[B]) = Q_{3,0}\left(y, \left[F_{k_{min}}^{(2)}\right], \left[Y_{k_{min}}^{(2)}\right]\right)$ otherwise $\breve{\varphi}(y,1,0,[A],[B]) = Q_{3,0}\left(y, \left[F_0^{(2)}\right], \left[Y_0^{(2)}\right]\right)$. Under condition $y\ge y_n$ or under conditions $y\in[y_{n-1}, y_n]$ and $y\notin[y_k, y_{k+1}]$ where $k=\overline{0,n-2}$ $\breve{\varphi}(y,2,1,[A],[B]) = P_2\left(y, \left[F_{n-2}^{(2)}\right], \left[Y_{n-2}^{(2)}\right]\right)$ otherwise if $y\notin[y_0, y_1]$ and $y\in\left[y_{k_{min}}, y_{k_{min}+1}\right]$ where k_{min} is the smallest between integer numbers k such that $1\le k\le n-2$ and $y\in[y_k, y_{k+1}]$, then $\breve{\varphi}(y,2,1,[A],[B]) = Q_{5,1}\left(y, \left[F_{k_{min}-1}^{(3)}\right], \left[Y_{k_{min}-1}^{(3)}\right]\right)$ otherwise

$$\breve{\varphi}(y,2,1,[A],[B]) = P_2\left(y, \left[F_0^{(2)}\right], \left[Y_0^{(2)}\right]\right). \tag{25}$$

If $y\ge y_n$ or if for any integer k such that $0\le k\le n-3$ $y\notin[y_k, y_{k+1}]$ and $y\in[y_{n-2}, y_{n-1}]$ or if for any integer k such that $0\le k\le n-2$ $y\notin[y_k, y_{k+1}]$ and $y\in[y_{n-1}, y_n]$, then $\breve{\varphi}(y,2,0,[A],[B]) = P\left(y, \left[F_{n-2}^{(2)}\right], \left[Y_{n-2}^{(2)}\right]\right)$ otherwise if $y<y_n$ and $y\in\left[y_{k_{min}}, y_{k_{min}+1}\right]$ where k_{min} is the smallest between the integer numbers k such that $0\le k\le n-3$ and $y\in[y_k, y_{k+1}]$, then $\breve{\varphi}(y,2,0,[A],[B]) = Q_{5,0}\left(y, \left[F_{k_{min}}^{(3)}\right], \left[Y_{k_{min}}^{(3)}\right]\right)$ otherwise $\breve{\varphi}(y,2,0,[A],[B]) = Q_{5,0}\left(y, \left[F_0^{(3)}\right], \left[Y_0^{(3)}\right]\right)$.

From Eqs. (3), (9), (10) and these definitions of the functions $\breve{\varphi}(y,1,0,[A],[B])$ and $\breve{\varphi}(y,2,j,[A],[B])$ where $j=\overline{0,1}$ it follows that if the interpolation nodes are arranged in the increasing order, then

$$\breve{\varphi}\left(a+b-y,1,0,\left[\tilde{A}\right],\left[\tilde{B}\right]\right) = \varphi(y,1,1,[A],[B]), \tag{26}$$

$$\breve{\varphi}(y,1,0,[A],[B]) = \varphi(y,1,0,[A],[B]), \tag{27}$$

$$\breve{\varphi}\left(a+b-y,2,0,\left[\tilde{A}\right],\left[\tilde{B}\right]\right)=\varphi(y,2,2,[A],[B]), \tag{28}$$

$$\breve{\varphi}\left(a+b-y,2,1,\left[\tilde{A}\right],\left[\tilde{B}\right]\right)=\varphi(y,2,1,[A],[B]), \tag{29}$$

$$\breve{\varphi}(y,2,1,[A],[B])=\varphi(y,2,1,[A],[B]),\ \breve{\varphi}(y,2,0,[A],[B])=\varphi(y,2,0,[A],[B]), \tag{30}$$

Theorem 5. If interpolation nodes are distributed chaotically, then in the general case $\breve{\varphi}(y,2,1,[A],[B])\neq\breve{\varphi}\left(a+b-y,2,1,\left[\tilde{A}\right],\left[\tilde{B}\right]\right)$.

Proof. To prove the theorem let us consider the following example. Let us assume that $n=5$, $a=0$, $b=2$, $h=0.4$, $y_0=0$, $y_i=(i+1)\cdot h$, $i=\overline{1,3}$, $y_4=h$, $y_5=2$, $f(y)=(y-2)+e^2-e^y$ where $0\le y\le 2$. According to Eq. (7) $\tilde{y}_0=0$, $\tilde{y}_1=2-h$, $\tilde{y}_i=2-(6-i)\cdot h$ where $i=\overline{2,4}$, $\tilde{y}_5=2$. If $y=3h/2$, then according to Eq. (6) $\tilde{y}=2-3h/2$. Since $y_0\le y\le y_1$ and $\tilde{y}_0\le\tilde{y}\le\tilde{y}_1$, from Eq. (25) and an explicit form of an interpolation polynomial [14] it follows that

$$\breve{\varphi}(y,2,1,[A],[B])=P_2\left(y,\left[F_0^{(2)}\right],\left[Y_0^{(2)}\right]\right)\approx 4.19, \tag{31}$$

$$\breve{\varphi}(\tilde{y},2,1,\left[\tilde{A}\right],\left[\tilde{B}\right])=P_2\left(\tilde{y},\left[\tilde{F}_0^{(2)}\right],\left[\tilde{Y}_0^{(2)}\right]\right)\approx 4.32, \tag{32}$$

From Eqs. (31) and (32) it follows that in the general case $\breve{\varphi}(y,2,1,[A],[B])\neq\breve{\varphi}\left(a+b-y,2,1,\left[\tilde{A}\right],\left[\tilde{B}\right]\right)$. The theorem is proved.

Remark 4. Here we assume that the interpolation nodes are arranged in the order of increasing. From Eq. (3) it follows that if $y\in[y_0,y_2]$ $\left(y\in[y_{n-2},y_n]\right)$, then for each integer j such that $0\le j\le 2$ $\varphi(y,2,j,[A],[B])$ depends only on y, y_i, and $f(y_i)$ where $i=\overline{0,4-j}$ $\left(i=\overline{n-2-j,n}\right)$. Thus, according to Definition 1 $\varphi(y,2,2,[A],[B])$ is strongly local in the vicinity of the point $y=a$ while $\varphi(y,2,0,[A],[B])$ is strongly local in the vicinity of the point $y=b$. From Definition 1 and Theorem 2 it follows that in the general case $\varphi(y,2,j,[A],[B])$ where $j=\overline{0,1}$ are not strongly local in the vicinity of the point $y=a$ while $\varphi(y,2,j,[A],[B])$ where $j=\overline{1,2}$ are not strongly local in the vicinity of the point $y=b$.

Remark 5. Here we assume that the interpolation nodes are arranged in the order of increasing. From Eq. (3) it follows that if $y\in[y_0,y_1]$ $\left(y\in[y_{n-1},y_n]\right)$, then for each integer j such that $0\le j\le 1$ $\varphi(y,1,j,[A],[B])$ depends only on y, y_i, and $f(y_i)$ where $i=\overline{0,2-j}$ $\left(i=\overline{n-1-j,n}\right)$. Thus, according to Definition 1 $\varphi(y,1,1,[A],[B])$ is strongly local in the vicinity of the point $y=a$ while $\varphi(y,1,0,[A],[B])$ is strongly local in the vicinity of the point $y=b$. From Definition 1 and Theorem 2 it follows that in the general case $\varphi(y,1,1,[A],[B])$ is not strongly local in the vicinity of the point $y=b$ while $\varphi(y,1,0,[A],[B])$ is not strongly local in the vicinity of the point $y=a$.

Remark 6. It follows from Eqs. (4)–(6) and Theorem 1 that the splines $\varphi(y,s,j,[A],[B])$ where $s=\overline{1,n-1}$ and $j=\overline{0,s}$ at any point of the interpolation segment depend on values of the interpolated function in no more than $s+2$ nodes. As for the splines $g(y,m,[A],[B])$ where $m=\overline{1,4}$, from Eqs. (17)–(23) it follows that in the general case at any point of the interpolation segment these splines depend on values of the interpolated function in all nodal points.

Assuming that a_p, b_p^m, c_p^m, and d_p^m where $p=\overline{1,n}$ and $m=\overline{1,4}$ are calculated according to Eqs. (18)–(23), we can interpolate the free surface on every time layer by functions defined as follows.

Under condition $y > y_n$ or under conditions $y \in [y_{n-1}, y_n]$ and $y \notin [y_k, y_{k+1}]$ where $k = \overline{0, n-2}$ $\breve{g}(y, m, [A], [B]) = a_n + b_n^m (y - y_{n-1}) + c_n^m (y - y_{n-1})^2 + d_n^m (y - y_{n-1})^3$ otherwise if $y \le y_n$ and $y \in [y_{\tilde{k}-1}, y_{\tilde{k}}]$ where $\tilde{k}$ is the smallest between such the integer numbers k that $1 \le k \le n-1$ and $y \in [y_{k-1}, y_k]$, then $\breve{g}(y, m, [A], [B]) = a_{\tilde{k}} + b_{\tilde{k}}^m (y - y_{\tilde{k}-1}) + c_{\tilde{k}}^m (y - y_{\tilde{k}-1})^2 + d_{\tilde{k}}^m (y - y_{\tilde{k}-1})^3$ otherwise $\breve{g}(y, m, [A], [B]) = a_1 + b_1^m (y - y_0) + c_1^m (y - y_0)^2 + d_1^m (y - y_0)^3$. If $y \ge y_{n-1}$, then $\breve{\varphi}(y, 3, 2, [A], [B]) = P_3\left(y, \left[F_{n-3}^{(3)}\right], \left[Y_{n-3}^{(3)}\right]\right)$ otherwise if $y > y_2$ and $y \in [y_{\tilde{k}}, y_{\tilde{k}+1}]$ where $\tilde{k}$ is the smallest between such the integer numbers k that $2 \le k \le n-2$ and $y \in [y_k, y_{k+1}]$, then $\breve{\varphi}(y, 3, 2, [A], [B]) = Q_{7,2}\left(y, \left[F_{\tilde{k}-2}^{(4)}\right], \left[Y_{\tilde{k}-2}^{(4)}\right]\right)$ otherwise $\breve{\varphi}(y, 3, 2, [A], [B]) = P_3\left(y, \left[F_0^{(3)}\right], \left[Y_0^{(3)}\right]\right)$.

From Eqs. (3), (17), and the definitions of the functions $\breve{\varphi}(y, 3, 2, [A], [B])$ and $\breve{g}(y, m, [A], [B])$ given above where $m = \overline{1,4}$ it follows that if the interpolation nodes are arranged in the order of increasing $(a = y_0 < y_1 < \ldots < y_n = b)$, then the following equalities hold

$$\breve{\varphi}(y, 3, 2, [A], [B]) = \varphi(y, 3, 2, [A], [B]), \quad \breve{g}(y, m, [A], [B]) = g(y, m, [A], [B]). \tag{33}$$

Results of numerical experiments. We take the values of input parameters from [10], [11] for the first two set ups and from [8], [11] for the last two ones. They correspond to real scale grouting. In what follows analyzing numerical solutions we estimate the value of the measure of a difference between two splines $f_1(y)$ and $f_2(y)$ that interpolate final injection front positions according to Eq. (1). Demchuk [11] presents results of 10 calculations of final injection front positions. Calculations # 1 and # 2 are performed in the frameworks of models of the first type and correspond to set ups # 1 and # 2 respectively. Calculations # 3 and # 4 are performed in the frameworks of models of the first type and correspond to set up # 3 as well as to respectively the cases of the most rigid deformable soil and the softest one. Calculations # 5 and # 6 are performed in the frameworks of models of the first type and correspond to set up # 4 as well as to respectively the cases of the most rigid deformable soil and the softest one. In their turn, calculations # 7 and # 8 are performed in the framework of models of the second type and correspond to set up # 3 and respectively the cases of the most rigid deformable soil and the softest one. Finally, calculations # 9 and # 10 are performed in the frameworks of models of the second type and correspond to set up # 4 and respectively the cases of the most rigid soil and the softest one. In Table 1 ε_i is the estimation of the truncation error of calculation # i where $i = \overline{1,10}$ Demchuk [11] obtains neglecting the contributions of the uncertainties in the final injection front position due to uncertainties in the choice of the method of free surface interpolation on every time layer. Performing calculations Demchuk [11] uses the function $\breve{\varphi}(y, 2, 1, [A], [B])$ to interpolate the free surface on every time layer.

Table 1

Measures of the difference between the final injection front position we obtain interpolating the free surface on every time layer by different functions and the respective ones Demchuk [11] obtains

i	ε_i, %	$\delta_i^{(1,0)}$, %	$\delta_i^{(1,1)}$, %	$\delta_i(0.7)$, %	$\delta_i(0.002)$, %	$\tilde{\varepsilon}_i(0.002)$, %
1	3.2	25.5	15.0	2.98	0.05	3.20
2	5.5	19.7	9.94	5.02	0.02	5.50
3	5.4	36.8	31.5	12.00	0.66	5.44
4	5.5	36.3	30.7	11.26	0.59	5.53
5	7.4	28.19	36.93	2.57	0.10	7.40
6	7.1	28.43	36.71	2.28	0.08	7.10
7	4.2	31.89	18.43	6.16	0.28	4.21
8	4.2	31.87	18.23	3.67	0.15	4.20
9	4.7	20.8	25.9	4.43	0.01	4.70
10	4.3	21.8	26.6	3.58	0.01	4.30

Numerical verification of the assumption that we can neglect the uncertainty in the final injection front position due to the uncertainty in the choice of the method of free surface interpolation on every time layer, estimating the truncation error of calculation # i where $i = \overline{1,10}$, is presented in section 2. To find additional one in what follows we will conduct an analysis of numerical solutions having in mind that this assumption is correct. If we do not arrive at any inconsistency, we will have the new numerical verification of this assumption. The aim of this analysis is to find the function for the interpolation of the free surface on every time layer as good as the one that coincides with $\varphi(y, 2, 1, [A], [B])$ when nodes are arranged in the increasing order. As candidates we consider functions using which we can obtain final injection front position in all ten cases we consider. Results of numerical calculations indicate that we can not obtain the final injection front position in at least 5 out of ten calculations defined above interpolating the free surface on every time layer by one of the following functions: $\breve{\varphi}(y, 2, 0, [A], [B])$, $\breve{\varphi}(a + b - y, 2, 0, [\tilde{A}], [\tilde{B}])$, $\breve{\varphi}(y, 3, 2, [A], [B])$, $\breve{g}(y, m, [A], [B])$ where $m = \overline{2,4}$ and in calculations # 1 and # 2 interpolating the injection front on every time layer by the function $\breve{g}(y, 1, [A], [B])$. It can be explained by the following:

1. According to Remark 4 the spline $\varphi(y, 2, 0, [A], [B])$ is strongly local in the vicinity of the point E and in the general case the spline $\varphi(y, 2, 1, [A], [B])$ is not strongly local in this vicinity. Therefore, from Eqs. (30) it follows that our failure to obtain the final injection front position in at least 5 out of ten calculations defined above interpolating the free surface on every time layer by $\breve{\varphi}(y, 2, 0, [A], [B])$ indicate that the possible distortions of the free surface mentioned in Remark 3 do occur. Hence, the curvilinear grids these calculations performed on do have chaotic dispositions of their nodes on some time layers. It provides the possible explanation of our numerical result regarding not considering the function $\breve{\varphi}(y, 2, 0, [A], [B])$ as the candidate to be the needed function. In what follows we assume that the possible distortion of the free surface mentioned in Remark 3 occurs in each calculation we perform.
2. According to Remark 1 the function which plot is the free surface is distorted in the vicinity of the point O. The spline $\varphi(y, 2, 2, [A], [B])$ is strongly local in this vicinity while in the general case the spline $\varphi(y, 2, 1, [A], [B])$ is not (see Remark 4). It follows from Eq. (28) and the first equation of Eqs. (30) that the distortion of the function which plot is the free surface in the vicinity of the point O is stronger when the injection front is interpolated by $\breve{\varphi}(a + b - y, 2, 0, [\tilde{A}], [\tilde{B}])$ than when it is interpolated by $\breve{\varphi}(y, 2, 1, [A], [B])$. This observation verifies the validity of our numerical result regarding not considering the function $\breve{\varphi}(a + b - y, 2, 0, [\tilde{A}], [\tilde{B}])$ as the candidate to be the needed function.
3. According to Remark # 2 the spline $\varphi(y, 3, 2, [A], [B])$ is not strongly local in the vicinities of the points O and E. Therefore, it is unlikely that the distortions of the free surface in the vicinities of the points O and E cause our failure to obtain the final injection front positions in some of above mentioned 10 cases when we interpolate the free surface on every time layer by the function $\breve{\varphi}(y, 3, 2, [A], [B])$. It follows from Eqs. (3)–(5) and Theorem 1 that the spline $\varphi(y, s, j, [A], [B])$ where $0 < s \le n - 1$ and $0 \le j \le s$ is fully determined by interpolation polynomials of the order s. The sensitivity of an interpolation polynomial to the errors in the values of the interpolated function in the interpolation nodes increases with the increase in its degree. Riabenkii [14] states that the interpolation polynomials of degree greater than 3 are really used in practice due to this effect. Therefore, the first equation of Eqs. (33), the first equation of Eqs. (30), and the fact that the sensitivities of the splines $\varphi(y, 3, j, [A], [B])$ where $j = \overline{0,3}$ to the errors in the values of the interpolated function in interpolation nodes are likely to be higher than that of the spline

$\varphi(y, 2, 1, [A], [B])$ suggest ignoring the consideration of not only the function $\breve{\varphi}(y, 3, 2, [A], [B])$ but also any function that in the case of the interpolation node arrangement in the increasing order coincides with one of splines $\varphi(y, s, j, [A], [B])$ where $s \geq 3$ and $j = \overline{0,s}$ as candidates to be the needed function.

4. From Remarks 1, 3, and 6, the second equation of Eqs. (33), and the first equation of Eqs. (30) it follows that it is likely that the function $\breve{\varphi}(y, 2, 1, [A], [B])$ better interpolates the injection front on parts of the interpolation segment not situated in the vicinity of the point O or in the vicinity of the point E than $\breve{g}(y, m, [A], [B])$ where $m = \overline{1,4}$ do. This observation verifies the validity of our numerical results regarding not considering the functions $\breve{g}(y, m, [A], [B])$ where $m = \overline{1,4}$ as candidates to be the needed function.

As mentioned above the function $\breve{g}(y, 1, [A], [B])$ performs better interpolating the free surface on every time layer than each one of the functions: $\breve{\varphi}(y, 2, 0, [A], [B])$, $\breve{\varphi}(a + b - y, 2, 0, [\tilde{A}], [\tilde{B}])$, $\breve{\varphi}(y, 3, 2, [A], [B])$, $\breve{g}(y, m, [A], [B])$ where $m = \overline{2,4}$. Since according to Riabenkii [14] the spline $\varphi(y, 2, 1, [A], [B])$ is the most interesting for practical applications, there is a temptation to consider the function $\alpha \cdot \breve{g}(y, 1, [A], [B]) + (1 - \alpha) \cdot \breve{\varphi}(y, 2, 1, [A], [B])$ where $0 \leq \alpha \leq 1$ as the candidate to be the needed function. If we perform calculation # i of the final injection front positions, interpolating the free surface on every time layer by the functions $\breve{\varphi}(y, 1, 0, [A], [B])$, $\breve{\varphi}(a + b - y, 1, 0, [\tilde{A}], [\tilde{B}])$, $\breve{\varphi}(a + b - y, 2, 1, [\tilde{A}], [\tilde{B}])$, and $\alpha \cdot \breve{g}(y, 1, [A], [B]) + (1 - \alpha) \cdot \breve{\varphi}\{y, 2, 1, [A], [B])$, then the measure of the difference between each one of these positions and the respective position Demchuk [11] obtains we respectively denote as $\delta_i^{(1,0)}$, $\delta_i^{(1,1)}$, $\delta_i^{(2,1)}$, and $\delta_i(\alpha)$ where $i = \overline{1,10}$. In calculation # 1 we can not obtain the final injection front position interpolating the free surface on every time layer by the function $0.8 \cdot \breve{g}(y, 1, [A], [B]) + 0.2 \cdot \breve{\varphi}(y, 2, 1, [A], [B])$. We obtain that $\delta_i^{(2,1)} \leq 0.01\%$ where $i = \overline{1,10}$ and the values of $\delta_i^{(1,0)}$, $\delta_i^{(1,1)}$, and $\delta_i(\alpha)$ where $i = \overline{1,10}$ presented in Table 1. Since on every time layer Demchuk [11] interpolates the free surface by the function $\breve{\varphi}(y, 2, 1, [A], [B])$, from Eq. (29) and the first equation of Eqs. (30) it follows that we can not estimate the uncertainty in the final injection front position obtained in calculation # i due to the uncertainty in the choice of the method of free surface interpolation on every time layer as $\delta_i^{(2,1)}$ where $i = \overline{1,10}$. Since $\delta_i(0.7) < \delta_i^{(1,1)}$ and $\delta_i(0.7) < \delta_i^{(1,0)}$ where $i = \overline{1,10}$, we can assert that it is better to use the function $0.7 \cdot \breve{g}(y, 1, [A], [B]) + 0.3 \cdot \breve{\varphi}(y, 2, 1, [A], [B])$ than either $\breve{\varphi}(y, 1, 0, [A], [B])$ or $\breve{\varphi}(a + b - y, 1, 0, [\tilde{A}], [\tilde{B}])$ to interpolate the free surface on every time layer. Using Eqs. (26), (27), Remarks # 1, 3, and 5 we conclude that it is likely that the free surface is more distorted in the vicinities of the points O and E when it is interpolated by the function $\breve{\varphi}(y, 1, 0, [A], [B])$ or $\breve{\varphi}(a + b - y, 1, 0, [\tilde{A}], [\tilde{B}])$ than when it is interpolated by the function $0.7 \cdot \breve{g}(y, 1, [A], [B]) + 0.3 \cdot \breve{\varphi}(y, 2, 1, [A], [B])$. This conclusion verifies the validity of our numerical results regarding not considering functions $\breve{\varphi}(y, 1, 0, [A], [B])$ and $\breve{\varphi}(a + b - y, 1, 0, [\tilde{A}], [\tilde{B}])$ as candidates to be the needed function. From Table 1 it follows that $\delta_3(0.7) \approx \delta_4(0.7)$, $\delta_3(0.7)/2 > \delta_i(0.7)$, and $\delta_4(0.7)/2 > \delta_i(0.7)$ where $i = \overline{1,2,5,10}$. Total truncation error of the numerical calculation is estimated as square root of the sum of squares of errors from different sources [16]. Therefore, to find the needed

function on the segment $[0, 0.7]$ we will find the value of α at which $|\tilde{\varepsilon}_i(\alpha) - \varepsilon_i| < 0.1$ where $\tilde{\varepsilon}_i(\alpha) = \sqrt{(\delta_i(\alpha))^2 + (\varepsilon_i)^2}$ and $i = \overline{3,4}$. In Table 2 we present values of $\delta_i(\alpha)$ and $\tilde{\varepsilon}_i(\alpha)$ where $i = \overline{3,4}$ at different values of α from the segment $[0, 0.7]$. It follows from Table 2 that the function $\alpha \cdot \breve{g}(y, 1, [A], [B]) + (1-\alpha) \cdot \breve{\varphi}(y, 2, 1, [A], [B])$ can be used for the interpolation of the free surface on every time layer only if $0 \le \alpha \le 0.002$. Since $\delta_3(0.7)/2 > \delta_i(0.7)$ and $\delta_4(0.7)/2 > \delta_i(0.7)$ where $i = \overline{1,2,5,10}$, we should expect that $|\tilde{\varepsilon}_i(0.002) - \varepsilon_i| < 0.1$ where $\tilde{\varepsilon}_i(0.002) = \sqrt{(\delta_i(0.002))^2 + (\varepsilon_i)^2}$ and $i = \overline{1,2,5,10}$. In Table 1 we present the values of $\delta_i(0.002)$ and $\tilde{\varepsilon}_i(0.002)$ where $i = \overline{1,10}$. It follows from Table 1 that $|\tilde{\varepsilon}_i(0.002) - \varepsilon_i| < 0.1$ where $i = \overline{1,10}$. Since there is no inconsistency in the presented analysis, $\tilde{\varepsilon}_i(0.002)$ can be used as an estimation of the truncation error of calculation # i where $i = \overline{1,10}$.

Demchuk [11] checks numerically hypothesis # 3 formulated in section 2 for all ten calculations. From the data presented in Table 1 it follows that $\delta_i^{(2,1)} << \tilde{\varepsilon}_i(0.002)$ where $i = \overline{1,10}$. From Eq. (29), the first equation of Eqs. (30), and Theorem 5 it follows that this fact gives the new numerical verification of hypothesis # 3 (see section 2).

Table 2

Determination of the value of α at which $\tilde{\varepsilon}_i(\alpha) \approx \varepsilon_i$ where $i = \overline{3,4}$

α	$\delta_3(\alpha)$, %	$\delta_4(\alpha)$, %	$\tilde{\varepsilon}_3(\alpha)$, %	$\tilde{\varepsilon}_4(\alpha)$, %
0.5	14.17	13.44	15.16	14.52
0.3	14.77	14.06	15.73	15.10
0.03	6.36	5.87	8.34	8.04
0.01	2.83	2.56	6.10	6.07
0.007	2.09	1.88	5.79	5.81
0.005	1.55	1.39	5.62	5.67
0.002	0.66	0.59	5.44	5.53

Conclusion. In this work we conduct the analysis of the results of the final injection front position calculations in the frameworks of real scale grouting models in which the injection front is the free surface, using the assumption that we can neglect the uncertainty in the final injection front position due to the uncertainty in the choice of the method of free surface interpolation on every time layer estimating the truncation error of each one of these calculations. Since we have not arrived at any inconsistency, this analysis provides numerical verification of this assumption. We perform calculations on curvilinear grids that on some time layers can have chaotic dispositions of their nodes. We show that if such the dispositions of the nodes occur, then they give rise to the distortion of the injection front in the vicinity of the point E shown on Figure 1 (a). Two important numerical observations are the following

1. Demchuk [11] obtains the final injection front position in ten different cases interpolating the injection front on every time layer by the function $\breve{\varphi}(y, 2, 1, [A], [B])$.
2. Between these cases there are the ones in which we can not obtain the final injection front position interpolating the free surface on every time layer by the function $\breve{\varphi}(a + b - y, 2, 0, [\tilde{A}], [\tilde{B}])$.

From Eqs. (30) and Remarks 3 and 4 it follows that these numerical observations indicate that the chaotic dispositions of the curvilinear grid nodes do occur on some time layers in some of these cases. In the above

mentioned analysis we estimate the measure of the difference between two final injection front positions according to Eq. (1). In each calculation considered in this paper if we interpolate the free surface on every time layer by functions that in the case of arrangement of interpolation nodes in the increasing orders coincide, then the measure of the difference between respective final injection front positions is much smaller than the respective truncation error. This fact provides the verification of the hypothesis that the chaos in a space distribution of nodes of the curvilinear grid on some time layers does not cause a significant distortion of the final injection front position.

We will compare results of real scale permeation grouting model calculations with field observations.

1. Moretrench. Grouting methods. New York, 2010. 2. Bouchelaghem F., Vulliet L. Mathematical and numerical filtration-advection-dispersion model of miscible grout propagation in saturated porous media // Int. J. Numer. Anal. Geomech. – 2001. – 25(12). – P. 1195–1227. 3. Chupin O., Saiyouri N., and Hicher P.-Y. The effects of filtration on the injection of cement-based grouts in sand columns // Trans. Porous. Med. – 2008. – 72(2). – P. 227–240. 4. Demchuk M. B. A model of a cement grout injection in a saturated porous medium with boundary conditions conforming to initial ones // Scientific notes of NaUKMA. – 2011. – 125. – P. 46–51. 5. Bouchelaghem F. Two large scale injection experiments and assessment of the advection-dispersion-filtration model // Géotechnque. – 2002. – 52(9). – P. 667–682. 6. Chupin O., Saiyouri N., and Hicher P.-Y. Modeling of a semi-real injection test in sand // Computers and Geotechniques. – 2009. – 36(6). – P. 1039–1048. 7. Maghous S., Saada Z., Dormieux L., Canou J., and Dupla J. C. A model for in situ grouting with account for particle filtration // Computers and Geotechnics. – 2007. – 34(3). – P. 164–174. 8. Demchuk M. B. Mathematical modeling of the process of injection of an astringent grout in a porous medium // Math. and Comp. Modeling: Collected Research Papers. Series of Phys & Math Sciences. – 2010. – 4. – P. 61–75. 9. Demchuk M. B. About real scale models of a cement grout injection at a constant pressure in a dry soil // Artif. Intellig. – 2011. – 2. – P. 122–130. 10. Vlasyuk A. P. and Demchuk M. B. Numerical solution of a problem of giving waterside structure foundation strength // Scientific Bulletin of Chelm, Section of Mathematics and Computer Science. – 2007. – 1. – P. 211–222. 11. Demchuk M. B. Adoption of the continuum approach in real scale grouting models // J. "Math. Mach. Syst." – 2013. – 3. – P. 170–177. 12. Demchuk M. B., Saiyouri N. A realization of the uncertainty uniformity principle in a grouting model // Math. and Comp. Modeling: Collected Research Papers. Series of Phys & Math Sciences. – 2012. – 7. – P. 77–92. 13. Godunov S. K., Prokopov G. P. About calculations of conformal mappings and construction of finite difference grids // J. Comp. Math. Math. Phys. – 1967. – 7(5). – P. 1031–1059. 14. Riabenkii V. S. Introduction into computational mathematics. M., 2000. 15. Bahvalov N. S., Zhydkov N. P., and Kobelkov G. M. Numerical methods. – M., 1987. 16. Taylor, J. R. Errors in indirect measurements. – M., 1985.